

## Chapter 2

# Decreasing the Disturbance Coupled to Amplifiers

Since the amplifier is often the first signal processing stage in a system, it is likely that it may be subjected to the highest levels of disturbance, although the signal level at its input is still low. The signal-to-error ratio (SER) may therefore be degraded severely and these losses in SER can not be compensated adequately by other signal processing stages. Therefore, this work concentrates on presenting design strategies for negative-feedback amplifiers with reduced EMI susceptibility. Moreover, it is assumed that the subsequent signal processing stages are less susceptible to disturbances, and that the disturbance level in these stages is lower.

Analysis is an important part of design. To analyze EM compatibility, the design is split in two parts: circuit components and interconnects (Reitsma 2005; Canavero et al. 1990). The (active) circuit components<sup>1</sup> are responsible for nonlinear distortion of signals and envelope detection, which is analyzed with network theory. The interconnects are mainly responsible for disturbing signal transport, which is analyzed using electromagnetic field analysis. This chapter will present methods to estimate the disturbing signal in the interconnect(s) for a given EM environment, and measures for reducing this disturbance.

Section 2.1 presents a discussion about coupling of electromagnetic fields to the interconnects of negative-feedback amplifiers. Properties of the interconnect and their effect on the intended signal transfer is discussed in Sects. 2.2, 2.3, 2.4, and 2.5, while methods to estimate the amount of disturbance induced in an interconnect connected to an amplifier are presented in Sect. 2.6. The disturbance can be common-mode, which may be transferred to a differential-mode disturbance. This effect, and some measures for reducing common-mode disturbances are described in Sect. 2.7. Disturbances can also be reduced by using a conductive shield. Shield design is therefore discussed in Sect. 2.8. Finally, Sect. 2.9 presents the conclusions.

---

<sup>1</sup> Practical resistors, capacitors and inductors also show non-ideal behavior, specifically at higher frequencies. Their non-ideal behavior is extensively dealt with in textbooks, e.g., (Meijer 1996; Goedbloed 1993; Ott 2009), to which the interested reader is referred. Possible nonlinear behavior of passive components, e.g., electrolytic capacitors are not investigated, but may be analyzed with the methods presented in this work.

## 2.1 Coupling of Electromagnetic Fields

In principle EM-fields can be coupled to the negative-feedback amplifier by coupling to the source, the interconnect between the source and amplifier, the amplifier, the interconnect between the load and amplifier, the load, and the interconnect to the power supply as Fig. 2.1 shows. The resulting disturbance is depicted by voltage and current sources (Paul 1992). Source  $E_s$  may be a voltage or current signal source, and  $Z_L$  is the load impedance. Note that the depicted disturbance sources are differential-mode sources. Common-mode disturbances may also occur, but are not shown in Fig. 2.1.

Designing for low EMI susceptibility is equivalent to minimizing the disturbing sources and/or decreasing their adverse effect on the signal-to-error ratio (SER).

It may be expected that the loop formed by source, interconnect, and the input of the amplifier and the output loop consisting of the amplifier, interconnect, and load, respectively, are much better receptors for EM-fields than the amplifier. The latter usually has small dimensions and may be shielded or assumed to be shielded in the first design stages. Therefore, the design problem is simplified at this stage by assuming that interference picked up by the amplifier itself is negligible compared to that picked up by loops formed by the interconnects. The validity of this assumption has to be checked later in the design process and (if necessary) measures have to be taken to ensure that it is valid.

Interference reaching the amplifier via the input interconnect can not be distinguished from the intended signal when it is in the passband of the amplifier. For an ideal amplifier, no adverse effects exist when the disturbance is out-of-band. As was discussed in Chap. 1, practical amplifiers will show adverse effects that are quadratically dependent on the disturbing signal reaching its input.

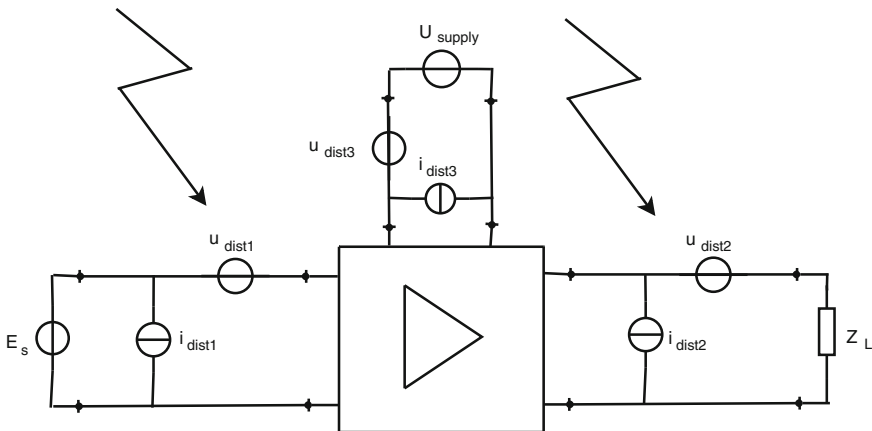


**Fig. 2.1** Interference coupling to an amplifier with source, load, power supply, and associated interconnects

For the ideal amplifier, interference pick-up at the output-load interconnect results in an addition of the disturbance to the load signal. Usually the disturbance is much smaller than the intended signal. Some of the disturbance will be transferred to the input in practical amplifiers, where its effect will be the same as in the case where interference is coupled directly to the input. The disturbance caused by interference at the output may be expected to be smaller compared to disturbance at the input, because some attenuation of the disturbance may be expected to occur in the transfer from output to input. Therefore, emphasis in this work is placed on the disturbance at the input of the amplifier, where its adverse effect is maximal.

In both the case of the ideal and the practical amplifier, the disturbing signal in the passband can not be distinguished from the information signal. Fortunately, a disturbance usually gets noticeable at higher frequencies, as will be shown in the next section. On top of that, measures to decrease the EM-coupling are usually effective at low frequencies and may become less effective at high frequencies (out-of-band). It may therefore be possible that the disturbance generated in the passband is still small enough to maintain the SER. The out-of-band interference may, however, cause deterioration of the SER.

In the remainder of this chapter we concentrate on determining the total disturbing signal at the input of an ideal amplifier. This disturbing signal gives the in-band SER to be expected directly and is also used in Chaps. 5 and 6 to determine the SER due to envelope detection.

Finally, interference may be coupled to the power supply interconnect. For a balanced power supply the resulting disturbance is balanced out and does not degrade the system performance. When the balancing is not ideal, or when there is no balancing at all, the disturbance may hamper system performance. For the power supply, however, the signal of interest (i.e., DC voltage/current) and the disturbance are well separated in the frequency domain. Filtering at low frequencies (e.g., a few Hz), is thus a powerful method to prevent disturbances on the power supply that hamper the SER.

### ***2.1.1 Coupling Mechanisms***

As was discussed earlier, the interconnects are responsible for transport of both the desired information and disturbance. The latter may also be called erroneous information or error(s) for short.

Errors in negative-feedback amplifiers can be divided in: errors due to noise, errors due to signal power, errors due to bandwidth limitations, and errors due to interference, as discussed in Chap. 1. Errors due to noise and signal power are mainly determined by the implementation of the negative-feedback amplifier. Apart from the negative-feedback amplifier bandwidth limitations and interference induced errors are also affected by the interconnect. The errors due to bandwidth limitations and interference caused by non-ideal behavior of the interconnects are discussed in this chapter.

An ideal interconnect does not have any resistance and does not receive or radiate electromagnetic fields. The ideal interconnect is commonly used in drawing schematics. It is just a line that forms a node for the various components connected to it, and it does not affect the signal transfer in any way. Real interconnects do affect the signal transfer, radiate and receive electromagnetic fields, and therefore a model describing these effects on the signal transfer is required. The model of the interconnect should be as simple as possible, yet it should be able to predict errors due to bandwidth limitations and interference caused by the interconnect with reasonable accuracy.

The resistance and loss of electromagnetic fields may cause bandwidth limitations and linear distortion to occur in interconnects. Reception of electromagnetic fields cause disturbances (errors) to be induced in the interconnect. In this work it is assumed that the interconnect has to be designed so that it does not introduce bandwidth limitations, i.e., it does not degrade the bandwidth specifications, and it does not introduce unacceptably large errors due to interference.

Simple models for the interconnect are presented in Sects. 2.2–2.6. These models can be used to analyze the generation of errors in the interconnect. They will be used to determine the remaining variables in the design of the interconnect such that for a given source, information domain and interference, a certain minimal SER can be maintained.

## 2.2 Electrical Model of the Interconnect

Any interconnect, whether it is a two-wire line, a coax cable, or a pair of traces on a printed circuit board, in essence is a two-port and thus shows a transfer between the input and output ports, and an impedance. The resistivity ( $\rho$ ) of the conductor material causes the conductors to have a resistance that depends on the dimensions of the interconnect. The skin effect causes an ‘AC’ component to occur in the resistance that increases with the square root of the frequency (Paul 1992).

The current flowing in the conductor generates magnetic fields both around and inside the conductor, resulting in an external inductance (i.e., the self inductance) and an internal inductance, respectively. This internal inductance is usually negligible compared to the external inductance (Paul 1992). Charge distributed over the conductor surface result in an electric field, resulting in a capacitance. The resistance, capacitance and inductance of the interconnect may result in errors in the information transfer due to bandwidth constraints or when reflections of the signal occur.

Interconnects, and complete systems can, based on their dimensions, be divided in electrically-small and electrically-large interconnects. ‘Large’ in the case of interconnects (and even complete systems) means that the dimensions of the interconnect become comparable to or greater than the wavelength,  $\lambda$ , of the signal. For engineering purposes, an interconnect is electrically-large when it is larger or equal to  $\lambda/10$  (Goedbloed 1993). Smaller interconnects (i.e.,  $<\lambda/10$  in length) are regarded to be electrically-small. The signal may be both intended and parasitic due to a disturbance.

Note that the same interconnect can be small for the intended signal but large for the disturbance, or vice-versa. The latter is not considered in this work.

Coupling of a disturbance depends on the distance between the interference source and the receptor. Here, two cases can also be distinguished since the distance ( $d$ ) can be electrically-small or electrically-large. A distance is large when compared to the antenna size (Reitsma 2005);  $d \geq 2D^2/\lambda$ , with  $D$  being the maximum overall antenna dimension (Sinnema 1988). In the case of small dipoles, the distance becomes large at an approximate value of  $\lambda/(2\pi)$  (Goedbloed 1993). Distance  $d$  is then large when  $d \geq \lambda/(2\pi)$ . The latter boundary is usually used in EMC engineering.

When  $d$  is small, the coupling is considered near-field, and when  $d$  is large, a far-field coupling problem (Paul 1992; Goedbloed 1993). The near-field coupling can be represented by a coupling capacitance and a mutual inductance. This is not the case for far-field coupling as the electromagnetic wave propagation has to be considered in that case.

For the coupling of interference, four different situations can be distinguished. When we take the length  $\mathcal{L}$  of the interconnect as representative for the dimensions of the interconnect, we have (Reitsma 2005):

1. both  $\mathcal{L}$  and  $d$  are small
2.  $\mathcal{L}$  is small and  $d$  is large
3.  $\mathcal{L}$  is large and  $d$  is small
4. both  $\mathcal{L}$  and  $d$  are large

Case 1 results in coupling to a lumped element model representation of the interconnect via mutual inductance ( $M_{12}$ ) and a coupling capacitance ( $C_{12}$ ) (Paul 1992), see Fig. 2.2a. The distributed resistance of the interconnect is represented by a resistance ( $R$ ), the inductance and capacitance by  $L$  and  $C$ , respectively, and the conductance between the conductors by  $G$ . Coupling of disturbance via mutual inductance and coupling capacitance is often called crosstalk.

The second case (2, above) represents plane wave coupling to a small interconnect. In this work only the *receiving* small interconnect is considered. It is assumed that the designer can not do anything to reduce the interference generated by emitters at a large distance. The plane wave induces a voltage (represented by voltage source,  $u$ ) and a current (represented by current source,  $i$ ) in the lumped element model of the interconnect, as depicted in Fig. 2.2b. The plane wave is represented three vectors  $\vec{E}$ ,  $\vec{H}$ , and  $\vec{S}$ , being the electric field, the magnetic field, and the Poynting vector, respectively. The disturbance induced by the plane wave is represented by a single voltage ( $u$ ) and current source ( $i$ ) (Paul 1992). Estimating the effects of plane wave coupling on electrically-short interconnects is discussed in Sect. 2.6.1.

Case 3 gives coupling via distributed mutual inductance and coupling capacitance to transmission lines. In the case of transverse electromagnetic (TEM) field propagation, the fields have no component parallel to the uniform line conductors (Paul 1992; Sinnema 1988; Smith 1977). The model of an electrically-long interconnect suffering from near-field disturbance is shown in Fig. 2.2c (Reitsma 2005). The ‘uniform’ property of a transmission line refers to the constancy of the conductor

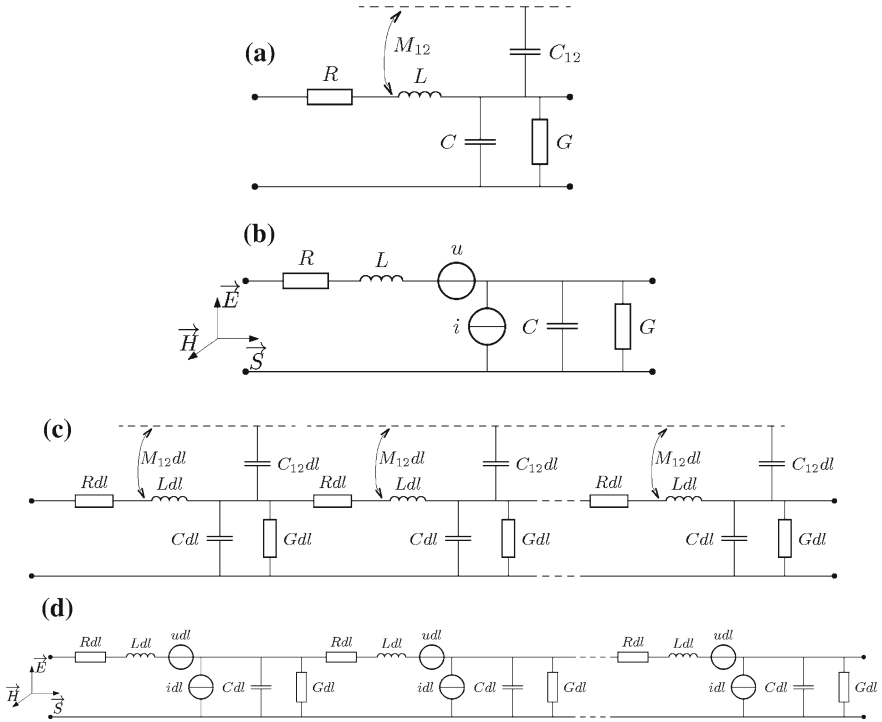


**Fig. 2.2** Representations of both electrically-small and large interconnects suffering from interference due to crosstalk (2.2a, 2.2c) and plane wave coupling (2.2b, 2.2d). **a** Lumped representation of an electrically short interconnect. Crosstalk is represented by a lumped capacitance  $C_{12}$  and mutual inductance  $M_{12}$  to an interference source, which is depicted by the dotted line. **b** Lumped representation of plane wave coupling to an electrically short interconnect. The disturbance induced by the plane wave can be represented by a voltage and current source. **c** A uniform electrically-long interconnect suffering from crosstalk can be modelled by a cascade of infinitesimal length ( $dl$ ) sections of the interconnect. **d** A uniform electrically-long interconnect suffering from plane wave interference can be modelled by a cascade of infinitesimal length ( $dl$ ) sections of the interconnect

geometry (spacing and cross-sectional area), conductor material, and the surrounding dielectric medium over the length of the line (Smith 1977). The interconnect and its electrical properties are represented by a cascade of small sections ( $dl$ ) of the interconnect. The same holds for the coupling parameters  $M_{12}$  and  $C_{12}$ .

Solving the transmission line equations (Paul 1992; Sinnema 1988; Smith 1977) results in the familiar expressions for the characteristic impedance ( $Z_0$ ) and the propagation constant ( $\gamma$ ). Equations for determining the crosstalk in electrically-long interconnects are presented in Paul (1992) and Reitsma (2005). In this work, we are interested in disturbance due to out-of-band interference. Since out-of-band interference is often caused by sources located far away, crosstalk is not discussed in this work. The interested reader is referred to literature for measures to decrease crosstalk, e.g., (Reitsma 2005; Paul 1992; Ott 2009).

Finally, case 4 often depends on solving Maxwell's equation numerically. For some specific cases, like coupling to an isolated resonant antenna, analytical results are available, e.g., (Orfanidis 2004; Sinnema 1988; King 1956). The coupling of electromagnetic waves to (cylindrical) antennas for various frequencies (i.e., also non-resonant frequencies) may be determined by approximate equations given in, e.g., (King 1956). In this work it is assumed that no isolated antennas (i.e., interconnects) occur. This means that a conductive (ground) plane is present at a small distance away from the interconnect. For this situation, analytical closed form equations exist (Smith 1977) and will be presented in Sect. 2.6.2. Equations that also take nonuniformities of the interconnect into account can be found in Haase (2005), but will not be presented here for reasons of simplicity.

Fig. 2.2d depicts the electrically-long interconnect that is subjected to a plane wave. The effects of an interfering plane wave are now represented by the combined effects of infinitesimal voltage and current sources ( $udl$  and  $idl$ , respectively) (Paul 1992). Section 2.6.2 presents equations giving the total amount of disturbing current or voltage at the terminals of the interconnect. The combined effect of all sources (and the characteristic impedance) is thus taken into account in these equations.

The (lumped model) parameters  $R$ ,  $L$ ,  $C$ , and  $G$  can be determined from the equations presented in Table 2.1. Conductance  $G$  may often be neglected in practical cases, since  $\omega C \gg G$ , and  $R$  may often be neglected because it is smaller than the source impedance in most practical cases. These conditions are assumed in the remainder of this chapter.

## 2.3 Intended Signal Transfer in Electrically-Small Interconnect

When the interconnect is electrically-small, its behavior can be modelled using lumped elements, as was shown in Sect. 2.2. However, the way the lumped components are connected depends on the terminating impedances. Since an interconnect can be terminated at both sides, there are two terminating impedances. The two terminating impedances result in four extreme cases: both  $Z_1$  and  $Z_2$  are low (e.g., a short circuit), both  $Z_1$  and  $Z_2$  are high (e.g., an open connect),  $Z_1$  is low and  $Z_2$  is high, and  $Z_1$  is high and  $Z_2$  is low. These four combinations result in four lumped models of the interconnect (see Fig. 2.3). Note that the lumped components are connected in such a way that their effect on the signal transfer is maximal.

When it is assumed that  $Z_1$  represents the impedance of the signal source and  $Z_2$  the load of the source (i.e., the input impedance of the amplifier), it may easily be identified that Fig. 2.3a represents the model of an interconnect of a current processing amplifier and Fig. 2.3b represents the model of an interconnect of a voltage processing amplifier. Figures 2.3c and d represent situations that usually will not occur in case of negative-feedback amplifiers. They may, however, occur when EMC measures are taken, e.g., a shielding conductor connected to the reference via short circuits ( $Z_1 = Z_2 = 0$ ), or a floating interconnect ( $Z_1 = Z_2 = \infty$ ).

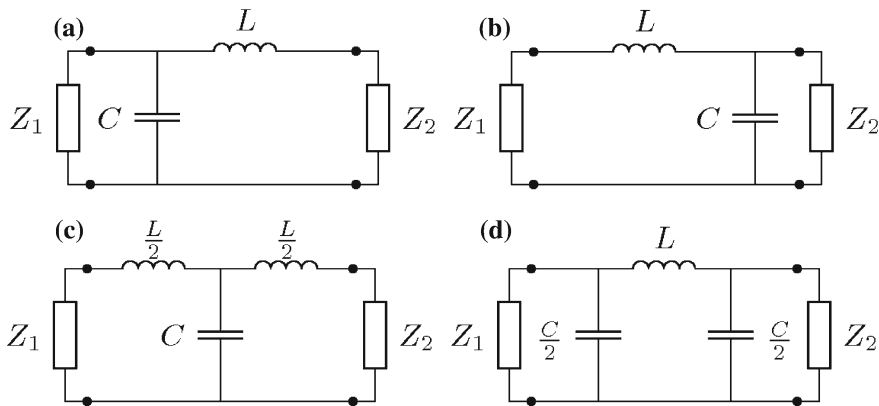


**Fig. 2.3** The lumped model that best represents the electrical behavior of an electrically-small interconnect depends on the terminating resistances. **a** Lumped model of interconnect in case  $Z_1$  is high and  $Z_2$  is low. **b** Lumped model of interconnect in case  $Z_1$  is low and  $Z_2$  is high. **c** Lumped model of interconnect in case  $Z_1$  and  $Z_2$  are both low. **d** Lumped model of interconnect in case  $Z_1$  and  $Z_2$  are both high

The inductance, capacitance, and resistance of the interconnect depend on its dimensions. The smaller the dimensions, the smaller the values of these lumped components become. The maximal dimensions of the interconnect therefore follow directly from the bandwidth requirement.

For example, consider a voltage domain information channel. Impedance  $Z_1$  is the source impedance and is taken to be the source resistance  $R_s$  for simplicity.  $Z_2$  is the input impedance of a voltage processing amplifier and is therefore ideally infinite. The transfer of the interconnect equals

$$H_u(s) = \frac{1}{s^2 LC + s(R_s C + \frac{L}{Z_2}) + 1 + \frac{R_s}{Z_2}} \approx \frac{1}{s^2 LC + s R_s C + 1}. \quad (2.1)$$

From this equation it follows that the bandwidth,  $B$ , of the transfer is estimated as<sup>2</sup>  $B \approx \frac{1}{2\pi R_s C}$  in most practical cases. For the bandwidth of the interconnect to have a negligible effect on the signal transfer and processing, it should be designed so that it is  $\geq 5$  times the bandwidth of the amplifier. From this requirement the maximal dimensions of the interconnect can be determined (see Sect. 2.5).

The solid line in Fig. 2.4 shows  $H_u$  of an electrically-short interconnect in case  $L$  equals  $1 \mu\text{H}$ ,  $C$  equals  $4 \text{ pF}$  and the source impedance is a resistance  $R_s$  of  $1 \text{ k}\Omega$ . The interconnect has no adverse effect on the signal transfer at low frequencies. The capacitance of the interconnect and the source resistance limit the bandwidth to

<sup>2</sup> When the current domain channel is evaluated, the same approximation for the bandwidth of the interconnect is found. The assumptions are now:  $Z_2$  is ideally zero, and when not zero much smaller than  $Z_1$ .  $Z_1$  is for simplicity also taken equal to the source resistance  $R_s$ .



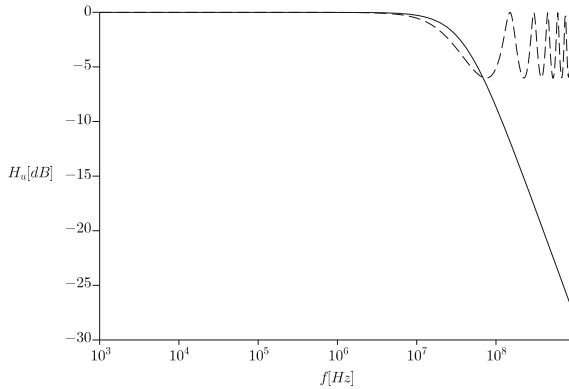


**Fig. 2.4** Transfers of two voltage domain channels with the same inductance and capacitance values ( $1 \mu\text{H}$  and  $4 \text{ pF}$ , respectively). The source impedance is  $Z_s = 1 \text{ k}\Omega$  and the amplifier's input impedance  $Z_{in} = \infty$ . The solid line depicts the Bode plot of the electrically-short channel. The dashed line depicts the Bode plot of an electrically-long channel with length  $\mathcal{L}$  of  $1 \text{ m}$  and  $Z_0 = 500 \Omega$

about  $39.8 \text{ MHz}$ . Transfer  $H_u$  decreases at a rate of  $20 \text{ dB/dec}$  for frequencies higher than the bandwidth.  $L$  does not affect  $H_u$  in the depicted frequency range.

## 2.4 Intended Signal Transfer in Electrically-Large Interconnect

The generally used name for a long interconnect is transmission line. The equations describing the behavior of long interconnects are therefore called transmission line equations. Both characteristic impedance,  $Z_0$  and propagation constant,  $\gamma$ , determine the behavior of an electrically large interconnect.

$Z_0$  is given by Sinnema (1988), Smith (1977):

$$Z_0 = \sqrt{\frac{R + j\omega L}{G + j\omega C}}. \quad (2.2)$$

The resistance per meter is given by  $R$ , the inductance per meter by  $L$ , the conductance per meter by  $G$ , and the capacitance per meter by  $C$ . For frequencies  $\omega L \gg R$  and  $\omega C \gg G$ , the characteristic impedance reduces to  $Z_0 = \sqrt{L/C}$ . Note that compared to an interconnect without insulation, the  $Z_0$  of an interconnect with insulation around the conductors is a factor  $\sqrt{\epsilon_r}$  lower, because  $C$  is the same factor larger.  $R$ ,  $G$ ,  $L$ , and  $C$  can be determined for various long interconnects with the equations presented in Sect. 2.5 (Table 2.1).

Propagation constant  $\gamma$  is defined as  $\sqrt{(R + j\omega L)(G + j\omega C)} = \alpha + j\beta$ , where  $\alpha$  is the attenuation constant and  $\beta$  is the phase constant of the transmission line. It

**Table 2.1** Overview of the parameters of some commonly used interconnects

|                            | R [ $\Omega/\text{m}$ ]   | G [S/m]                  | L [H/m]   | C [F/m]  |
|----------------------------|---|--------------------------|---|--|
| Two-wire line (Kaden 1959) | $\frac{\rho}{\pi \delta r_w} \frac{0.5d}{\sqrt{0.25d^2 - r_w^2}}$   | $\omega C \tan \delta_l$ | $\frac{\mu_0}{\pi} \ln \left( \frac{0.5d + \sqrt{0.25d^2 - r_w^2}}{r_w} \right)$  | $\frac{\pi \epsilon_{eff}}{\ln \left( \frac{0.5d + \sqrt{0.25d^2 - r_w^2}}{r_w} \right)}$              |
| Fig. 2.5a                  |   |                          |   |  |
| wire-plane                 | $\frac{\rho}{2\pi \delta r_w} \frac{0.5d}{\sqrt{0.25d^2 - r_w^2}}$<br>+ $\underbrace{\frac{\rho_p}{2\pi \delta_p \sqrt{0.25d^2 - r_w^2}}}_{\text{wire}}$<br>$\underbrace{\phantom{\frac{\rho_p}{2\pi \delta_p \sqrt{0.25d^2 - r_w^2}}}}_{\text{gnd-plane}}$ | $\omega C \tan \delta_l$ | $\frac{\mu_0}{2\pi} \ln \left( \frac{0.5d + \sqrt{0.25d^2 - r_w^2}}{r_w} \right)$<br>+ $\underbrace{\frac{\mu_0}{4\pi} \frac{\delta_p}{\sqrt{0.25d^2 - r_w^2}}}_{\text{gnd-plane}}; d = 2h$ | $\frac{2\pi \epsilon_{eff}}{\ln \left( \frac{0.5d + \sqrt{0.25d^2 - r_w^2}}{r_w} \right)}$<br>$d = 2h$ |
| Fig. 2.5b (Kaden 1959)     |   |                          |   |  |
| coax                       | $\frac{\rho_i \left( 1 + \frac{\delta_i}{2r_i} \right)}{2\pi r_i \delta_i} + \frac{\rho_a}{2\pi r_a \delta_a}$  | $\omega C \tan \delta_l$ | $r_i > \delta_i, d > \delta_a;$   | $\frac{2\pi \epsilon_0 \epsilon_r}{\ln \left( \frac{r_a}{r_i} \right)}$                                |
| Fig. 2.5c (Kaden 1959)     |   |                          | $\frac{\mu_0}{2\pi} \ln \left( \frac{r_a}{r_i} \right) + \frac{\mu_0}{4\pi} \left( \frac{\delta_i}{r_i} + \frac{\delta_a}{r_a} \right)$   |  |

Table 2.1 (continued)

|                | R [ $\Omega/\text{m}$ ]   | G [S/m]                  | L [H/m]  | C [F/m]  |
|----------------|---|--------------------------|--|--|
| two-wire coax  | $\approx \frac{\rho_t}{\pi r_t^2} \rho'_t +$  | $\omega C \tan \delta_1$ | $\approx \frac{\mu_0}{\pi} \left[ \ln \left( \frac{d(r_h^2 - (0.5d_1)^2)}{r_w(r_h^2 + (0.5d_1)^2)} \right) + 2 \frac{\delta}{r_h} \frac{(0.5d_1 r_h)^2}{r_h^4 - (0.5d_1)^4} \right]$ | $\frac{\pi \epsilon_0 \epsilon_r}{\ln \left( \frac{r_h^2 - (0.5d_1)^2}{r_w^2 + (0.5d_1)^2} \right) - A}$ |
| Fig. 2.5d      | $\frac{4\rho_h}{\pi r_h \delta_h} \frac{(0.5d_1 r_h)^2}{r_h^4 - (0.5d_1)^4} +$                                    |                          | $-\frac{\mu_0}{\pi} \left( \frac{r_w}{d_1} \right)^2 \left( 1 - \frac{(d_1 r_h)^2}{r_h^4 - (0.5d_1)^4} \right)^2 \lambda_z$  |  |
| (Kaden 1959)   | $\frac{\rho_i}{2\pi(0.5d_1)^2} \rho'_i \times$  |                          | $r_w < \delta : \lambda_z = \frac{1}{12} \left( \frac{r_w}{\delta} \right)^4$  | $A = \left( 1 - \frac{(d_1 r_h)^2}{r_h^4 - (0.5d_1)^4} \right)^2$  |
|                | $\left[ 1 - \frac{(d_1 r_h)^2}{r_h^4 - (0.5d_1)^4} \right]^2 ;$   |                          | $r_w > \delta : \lambda_z = 1 - \frac{\delta}{r_w}$  | $\times \left( \frac{r_w}{d} \right)^2$  |
|                | $r_l \leq 1.5\delta_i : \rho'_l \approx 1 + \frac{1}{48} \left( \frac{r_l}{\delta_l} \right)^4$                   |                          |  |  |
|                | $r_l \geq 1.5\delta_i : \rho'_l \approx \frac{1}{4} + \frac{r_l}{2\delta_i} + \frac{3\delta_l}{32r_l}$            |                          |  |  |
|                | $r_l < \delta_i : \rho'_z \approx \frac{1}{4} \left( \frac{r_l}{\delta_l} \right)^4$                              |                          |  |  |
|                | $r_l > \delta_i : \rho'_z \approx \frac{r_l}{\delta_l} - \frac{1}{2}$   |                          |  |  |
| Coplanar Strip | $2 \left( \frac{\rho}{w_t} + \frac{\rho}{2(\delta w + \delta t)} \right)$ (Paul 1992)                             | $\omega C \tan \delta_1$ | $\frac{\mu_0}{\pi} \left[ \ln \frac{\pi(d-w)}{w+t} + 1 \right]$ (Leferink 1995)  | $\epsilon_{eff} C_0$   |
| Fig. 2.5e      |   |                          |  | $C_0 = \frac{1}{c^2 L}$  |
| Microstrip     | $\left( \frac{\rho}{w t_f} + \frac{\rho}{2(\delta w + \delta t_f)} \right)$ (Paul 1992)                           | $\omega C \tan \delta_1$ | $\frac{\mu_0}{2\pi} \ln \left( \frac{2\pi h}{w + (1+\pi)t_f} + \frac{w+t_f}{w + (1+\pi)t_f} \right)$   | $\epsilon_{eff} C_0$   |
| line           | $+ \underbrace{\left( \frac{\rho}{w_g t_g} + \frac{\rho}{2(\delta w_g + \delta t_g)} \right)}_{\text{gnd-plane}}$ |                          | $+ \underbrace{\frac{\mu_0}{2\pi} \ln \left( \frac{\pi h}{w_g + (1+\pi)t_g} + \frac{w_g+t_g}{w_g + (1+\pi)t_g} \right)}_{\text{gnd-plane}}$  | $C_0 = \frac{1}{c^2 L}$  |
| Fig. 2.5f      |   |                          | (Leferink 2001)  |  |

gives a measure for the attenuation and phase shift that a signal experiences while traveling across the transmission line.

The attenuation constant  $\alpha$  represents dissipative losses in the conductors and in the dielectric medium and is for low loss lines given by  $\alpha = \frac{R}{2Z_0} + \frac{GZ_0}{2}$  (Smith 1977). Resistance  $R$  increases with the square root of the frequency due to the skin effect (see Table 2.1). The equation for  $\alpha$  is in Np/m. In dB/m it is  $20 \log e \times \alpha \approx 8.686\alpha$  (Sinnema 1988). The dielectric losses represented by  $G$  increase proportional to frequency. The phase constant  $\beta$  equals  $\omega\sqrt{LC} = \omega\sqrt{\mu_0\mu_r\epsilon_0\epsilon_r}$  (Sinnema 1988; Smith 1977).

At high frequencies,  $\alpha$  may be dominated by inhomogeneities in the cable construction giving much higher attenuation than that predicted by this simple equation. For example, the loss at mobile telecommunication frequencies is about 0.2–2 dB/m, but losses over 10 dB/m have also been reported (Flintoft 2013).

In electrically-large interconnects it is impossible to work in either voltage or current domain, because after traveling a quarter wavelength, a voltage becomes a current signal and vice-versa (Reitsma 2005). Since the power remains constant, power should be the domain of the information. Therefore, the impedances of the signal source ( $Z_s$ ), the interconnect, and the input of the amplifier ( $Z_{in}$ ) should match to ensure constant power transfer. The impedance of an electrically-large interconnect is called the characteristic impedance ( $Z_0$ ). When  $Z_s = Z_0 = Z_{in}$ , the interconnect is properly terminated (Smith 1977).

Ideally, the input impedances of voltage and current amplifiers are infinite and zero, respectively. Infinite or zero impedances prevent power transfer, and therefore the signal will be reflected, resulting in distortion.<sup>3</sup> To prevent this, the information channel should be terminated by adding, e.g., series or parallel resistances in the current and voltage domain channel, respectively, or by applying a dual-loop negative-feedback amplifier with input and output impedances matched to the impedance of the interconnect. However, matching the (input) impedance of the amplifier to the characteristic impedance of the interconnect has some drawbacks.

Firstly, the voltage or current source impedance ends up in the transfer of the amplifier. An inaccurate or even nonlinear source impedance, causes the transfer to be inaccurate. This should therefore be avoided.

Secondly, most information sources (should) operate either in the voltage or current domain and thus require either voltage or current domain transport of the signal, i.e., the source should be terminated either with an infinite or zero impedance in the frequency band of the information. Note that from this discussion follows that the signal source impedance usually does not match the characteristic impedance of the interconnect either.

For frequencies well above the passband, both terminating impedances could be made equal to the characteristic impedance by shunting the terminating impedance with a capacitively-coupled resistance of the appropriate value. This may have detrimental effects on the noise performance of an amplifier, so this should be carefully

---

<sup>3</sup> Practical amplifiers do not have either zero or infinite input impedance, but values much lower or higher than  $Z_0$  can be expected. Therefore, reflections will still occur.

checked. Besides, source impedances are often characterized by a capacitive behavior at high frequencies. This makes it hard to accomplish a proper termination. We therefore limit this work to voltage and current domain signal transport.

For illustration purposes, it is shown what the consequences are of employing an electrically-large interconnect for transferring a voltage-domain signal. A comparable discussion holds for the current-domain channel. The transfer of the large interconnect between the source to the input of the voltage amplifier,  $H_u$ , is (Smith 1977)

$$H_u = \frac{Z_0 Z_{in}}{(Z_0 Z_s + Z_0 Z_{in}) \cosh(\gamma \mathcal{L}) + (Z_0^2 + Z_s Z_{in}) \sinh(\gamma \mathcal{L})}, \quad (2.3)$$

with  $\gamma$  being the propagation constant,  $\mathcal{L}$  the length of the interconnect, and  $Z_0$  its characteristic impedance.  $Z_s$  and  $Z_{in}$  are the source impedance and the (ideally infinite) input impedance of the voltage amplifier, respectively.

The signal integrity may be seriously hampered in case of electrically-large interconnects. Because impedances  $Z_s$  and  $Z_{in}$  do not match the characteristic impedance of the transmission line, reflections occur in the interconnect. Transfer  $H_u$  now shows resonances and anti-resonances, instead of a smooth 20 dB/dec roll-off as in case of the short interconnect (see the dashed line in Fig. 2.4). Although not clearly visible in a Bode diagram, the sign of the voltage reaching the amplifier may even become opposite to the sign of the voltage at the source, causing severe errors.

The first resonance<sup>4</sup> occurs at the frequency at which the interconnect length equals a quarter of the wavelength of the information. The following resonance frequencies occur at odd multiples of this frequency;  $f_{res} = \frac{nc}{4\mathcal{L}}$ , with  $n = 1, 3, 5 \dots$ , and  $c$  being the speed of light. The attenuation of the information that occurs at the resonance frequencies depends on  $Z_0$ . Lower values of  $Z_0$  cause larger attenuation values than higher values of  $Z_0$ . At the anti-resonance frequencies ( $f_{anti-res} = \frac{nc}{4\mathcal{L}}$ , with  $n = 2, 4, 6 \dots$ ) the transfer from source to input voltage is about unity, when the attenuation constant is low.

To ensure signal integrity, interconnects should never become electrically-large with respect to the wavelength of the highest frequency of the information it has to transfer. The maximal dimension (length) of an interconnect should be designed to be smaller than  $\lambda/10$ . This limitation is not a problem for the amplifiers dealt with in this work. These special purpose negative-feedback amplifiers are assumed to have a moderate bandwidth, up to several tens of MHz.

## 2.5 Parameters of Interconnects

For small interconnects, the lumped model parameters are of importance, and for large interconnects the characteristic impedance and the propagation constant are of

<sup>4</sup> The same convention as in Sinnema (1988) is used. High impedance or parallel resonant comparable transfers are called anti-resonant, whereas low impedance or series resonant comparable transfers are called resonant.

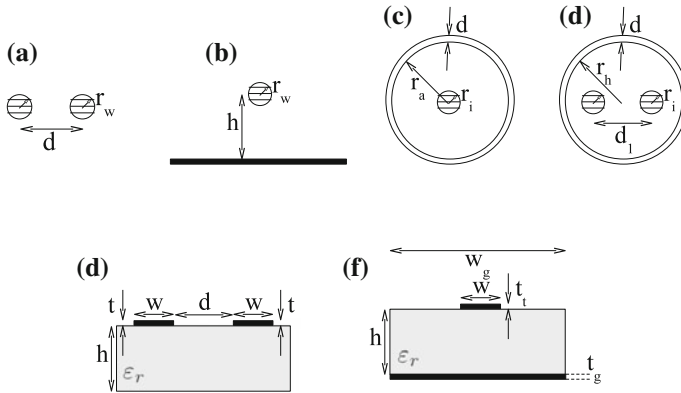


**Fig. 2.5** Some often encountered interconnects. **a** Two-wire line. **b** Wire over plane. **c** Coax. **d** Two-wire coax structure. **e** Coplanar strips. **f** Microstrip

importance. Deriving the equations for these parameters is beyond the scope of this work. Besides, these equations are presented in literature for several types of interconnects. For convenience, Fig. 2.5 shows some commonly encountered interconnects, and Table 2.1 presents equations for determining their parameters. More can be found in literature, e.g., (Leferink 2001; Leferink and van Doorn 1993; Leferink 1995; Reitsma 2005; Paul 1992; Kaden 1959).

In all equations for  $R$ , the skin depth (represented by  $\delta$ ) occurs. The skin depth is given by  $\delta = \sqrt{2\rho/(\mu\omega)}$  (Goedbloed 1993), with  $\rho$  being the resistivity of the conductor material,  $\omega$  the angular frequency and  $\mu = \mu_0\mu_r$ , with  $\mu_0$  being the permeability of free space, and  $\mu_r$  the relative permeability. The resistance thus increases with (the square root of the) frequency. In most practical cases, the external inductance (due to  $L$ ) will be larger than the frequency dependent part<sup>5</sup> of  $R$ , and therefore, the latter effect may thus be disregarded. An exception may be a broad microstrip line; its ‘AC’ resistance is not negligible to the external inductance (Leferink 1996).

Conductance  $G$  is calculated from the capacitance  $C$  and the loss tangent  $\tan \delta_1$  (third column of Table 2.1) (Orfanidis 2004). The latter represents the power loss of the dielectric of the insulating medium between the conductors. It is equal to  $\frac{1}{\rho\omega\epsilon_0\epsilon_r}$ , where  $\rho$  is the usually large specific resistance of the medium and  $\epsilon_r$  is the relative permittivity of the medium. When the medium is formed by a loss free medium, e.g., vacuum,  $\tan \delta_1$  equals zero. For an impression of the order of magnitude of a good insulator: the loss tangent  $\tan \delta_1$  of a typical polyethylene or teflon dielectric is of the order of 0.0004–0.0009 up to about 3 GHz (Orfanidis 2004). Conductance  $G$  will be much smaller than  $\omega C$  in practical cases, and may therefore be disregarded during design.

<sup>5</sup> The low resistivity of conductors cause a low value of  $R$  at DC, which increases with  $\sqrt{\omega}$ . Evaluation of the equations given in Table 2.1 shows that even for small distances between the conductors,  $\omega L$  is found to be much larger than the frequency dependent part of the resistance.

For the two-wire line and the wire over a (conductive) plane, holds that the distance between the conductors is represented by  $d$  or by the height  $h$  of the wire over the plane, and the radius of the wires by  $r_w$ , see Figs. 2.5a and b. The presented equation for the two-wire line (Table 2.1 row one) assume equal radii of the wires. The equations are valid under the assumption that  $d > r_w$ , skin depth ( $\delta$ ) is smaller than  $r_w$ , and height  $h$  is much higher than the skin depth ( $\delta_p$ ) of the ground plane (Kaden 1959).

For the coax cable and two-wire coax (Figs. 2.5c and d; Table 2.1 third and fourth row), hold that  $r_a$  and  $r_h$ , respectively, are the radii of the outer conductor,  $r_i$  is the radius of the inner conductor, and  $d_l$  is the distance between the two wires in the coax. The thickness of the outer conductor is represented by  $d$ . Note the constraints given in Table 2.1 for validity of the equations for the coax and two-wire coax.

When tracks on a printed circuit board are considered (the coplanar strips in Fig. 2.5e and the microstrip line in Fig. 2.5f; Table 2.1 fifth and sixth row), the width of the tracks is  $w$ ,  $t$  is the thickness of the track,  $w_g$  is the width of the ground plane, and  $h$  is the height of the printed circuit board material. The relative dielectric constant of the latter (typical glass-epoxy (Paul 1992)) is  $\epsilon_r$ . Note that the equations for calculating the inductance of the coplanar strips and the microstrip line hold when the length ( $\mathcal{L}$ ) of the track is much larger than  $d$  and  $w$  (Leferink 1995).

The effective permittivity  $\epsilon_{\text{eff}}$  in the equations for  $C$  (in rows 1, 2, 5, and 6), is determined by both the relative permittivity ( $\epsilon_r$ ) of the dielectric media (e.g., printed circuit board and wire insulation) and  $\epsilon_r \approx \epsilon_0$  of air, because the field lines penetrate both the air and the dielectric. Determining  $\epsilon_{\text{eff}}$  may be difficult, but some equations for determining it are presented in literature, e.g. (Sinnema 1988). For example, in case of a printed circuit board with  $w/h \ll 1$ ,  $\epsilon_{\text{eff}} \approx 0.5(\epsilon_r + 1)$ . More accurate and elaborate equations which are valid for other ratios of  $w$  and  $h$  are found in literature, e.g., (Sinnema 1988; Paul 1992). Parameter  $\epsilon_{\text{eff}}$  may, however, also easily follow from measurements. Note that parameter  $c$  for determining  $C_0$  (rows 5 and 6) is the speed of light in vacuum.  $C_0$  is the capacitance without the dielectric medium.

The equations presented in Table 2.1 are relatively simple and lend themselves to hand calculations. Moreover, they show the relation between the parameters  $R$ ,  $G$ ,  $L$ , and  $C$  and the physical dimensions of the interconnect, and can therefore be used in the first design steps. More accurate (and more elaborate) models, which can be used in the subsequent design steps are readily available in modern simulators.

## 2.6 Coupling of Interference to the Interconnect

When the distance between interfering source and receptor is large, the receptor is in the far field. The electric ( $\vec{E}$ ) and magnetic ( $\vec{H}$ ) fields of the electromagnetic wave are perpendicular to each other and perpendicular to the direction of propagation, which is represented by the Poynting vector  $\vec{S}$ , see Figs. 2.6 and 2.7. This electromagnetic wave is called a plane wave and has a constant ratio of the  $\vec{E}$  and  $\vec{H}$  fields: the wave impedance  $Z_w = E/H \equiv \sqrt{\mu_0/\epsilon_0} = 120\pi\Omega$  (Paul 1992).

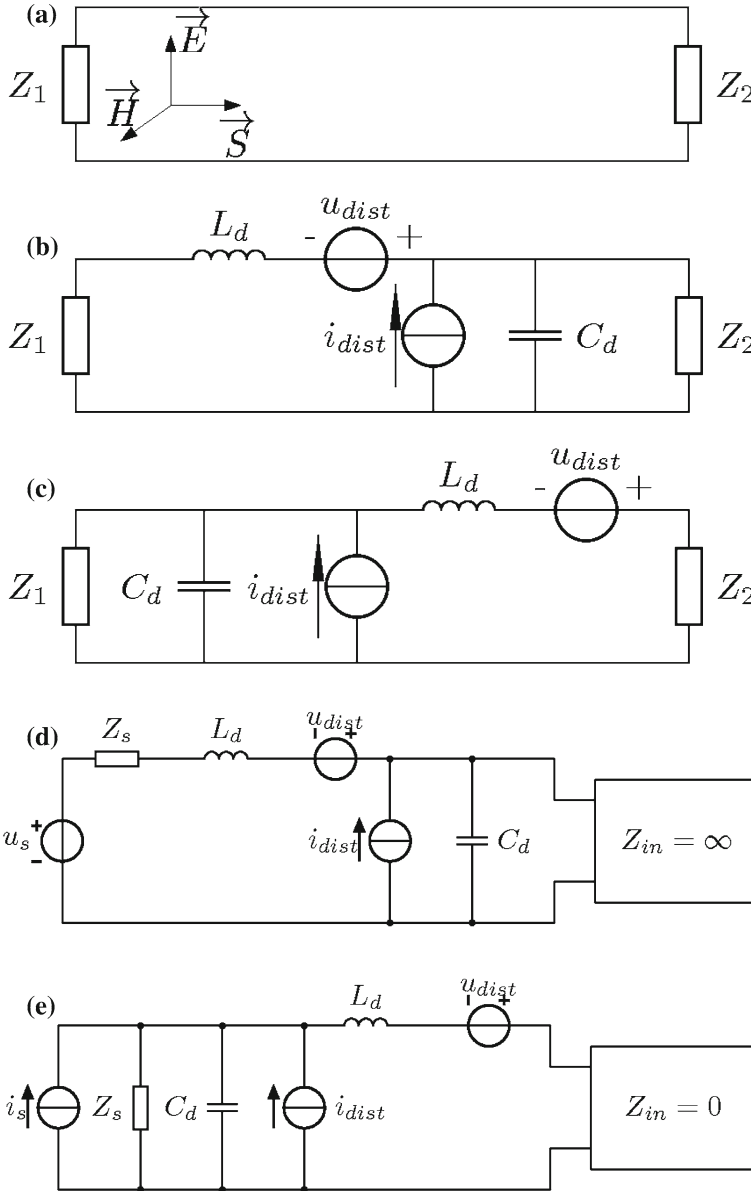


**Fig. 2.6** Representation of plane wave coupling to a two-wire line. Impedance of the wires are represented by lumped components. An electromagnetic plane wave induces a signal that can be represented by a voltage and a current source,  $u_{dist}$  and  $i_{dist}$ , respectively. **a** Two wire excited by an electromagnetic plane wave. **b** Best lumped model representation in case  $Z_1 < Z_2$ . **c** Best lumped model representation in case  $Z_1 > Z_2$ . **d** When the signal source supplies a signal voltage  $u_s$ , the input impedance of the amplifier should be infinite. **e** When the signal source supplies a signal current  $i_s$ , the input impedance of the amplifier should be zero



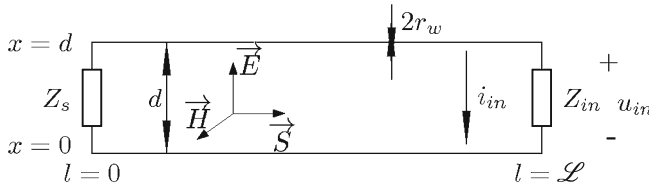


**Fig. 2.7** EM field coupling to an electrically-large interconnect. Note that the field may also have other orientations

In any interconnect (electrically short and long), disturbing signals are induced by interfering EM fields. These signals may be separated into antenna and transmission line currents (Leferink 2001). The antenna current is, by definition, the sum of all currents at any cross-section of a transmission line. Both differential-mode and common-mode currents are transmission line currents.

The transmission line currents, in a (multi-conductor) transmission line, can be found via transmission line theory (Paul 1992). A vital restriction is that the distance,  $d$ , between the conductors of the transmission line satisfies  $d \leq \frac{\lambda}{2\pi}$ , with  $\lambda$  being the wavelength of the highest interfering signal (Leferink 2001). Comparison of the far more elaborate antenna theory and this approach to determine the currents in a transmission line for spacings  $d \leq \frac{\lambda}{2\pi}$  (even up to  $\lambda/4$ ) show deviations between the two methods of less than 2 dB (Smith 1977), and therefore the transmission line theory can be used.

When the conductor is  $d > \frac{\lambda}{2\pi}$  far from a ground plane, the conductor has to be regarded as a monopole antenna (Leferink 2002). The antenna current at its terminal has to be determined with antenna theory. For determining the antenna current and antenna impedance as a function of frequency, the reader is referred to literature, e.g., (King 1956; King and Harrison 1969; Leferink 2001, 2002; Orfanidis 2004). In this work it is further assumed that all signal paths satisfy the earlier mentioned condition since most signal paths are not isolated. They are parallel, or approximately parallel, to a conducting (ground) plane (Smith 1977).

### 2.6.1 Plane Wave Coupling to Electrically-Short Interconnects

Figure 2.6a shows an two-wire interconnect subjected to a plane wave.<sup>6</sup> It is terminated on one side by impedance  $Z_1$  and on the other side by impedance  $Z_2$ . The electrical behavior of the two-wire line may be described by means of lumped-circuit models, i.e., an inductance ( $L_d$ ) and capacitance ( $C_d$ ), as is shown in Fig. 2.6b and c. Parameters  $L_d$  and  $C_d$  can be determined using the equations presented in Table 2.1.

The electric field component of the plane wave generates a current in the loop, while the magnetic field component induces a voltage in the loop Paul 1992. The generated current and voltage can be modelled by a current source in parallel with

<sup>6</sup> Plane wave coupling to other types of interconnects can be analyzed in the same way.

the impedances and a voltage source in series with the impedances (Paul 1992), respectively, as Fig. 2.6 shows.

Figure 2.6b shows the lumped element model for an electrically-short voltage domain channel that is subjected to a plane wave and Fig. 2.6c shows the current domain variant.

The magnitude of the disturbing signal sources generated by the electromagnetic field depends on the orientation of the two-wire line in the field. Depending on the angle between the two-wire line and the field, the induced signals may vary between some maximum and minimum value. In EMC engineering it is customary to assume the worse case: maximal magnitude of the induced signal. This also makes sense from a design point of view, so in this work maximal coupling is assumed.

The magnitude of the disturbing voltage at the input of the voltage processing amplifiers can easily be determined by assuming  $Z_{in}$  to be infinite (see Fig. 2.6d), and the magnitude of the disturbing current at the input of the current processing amplifier by assuming  $Z_{in}$  to be zero (see Fig. 2.6e). The intended signal sources ( $i_s$  and  $u_s$ , respectively) and the source impedance  $Z_s$  are also depicted in Fig. 2.6d and e. The signal source impedance will usually be composed of a resistance,  $R_s$ , shunted by a capacitance,  $C_s$ .

The practical negative-feedback amplifier will not have an infinite or zero input impedance. To simplify the design process, ideal amplifiers can be considered nevertheless. Deviations in the calculated disturbing signal due to deviations of  $Z_{in}$  from the ideal value presented to the input of the amplifier can be evaluated later. If the practical negative-feedback amplifier is designed properly, the constraints  $Z_s \ll Z_{in}$  in case of voltage processing amplifiers and  $Z_s \gg Z_{in}$  in case of current processing amplifiers, respectively, hold. The deviations between the ‘ideal’ and ‘practical’ values of the disturbing signal are therefore expected to be small.

When a current processing amplifier is considered, the input impedance approaches zero. Therefore, Fig. 2.6e should be used to determine the total disturbing signal. The total disturbing signal is the current flowing into the amplifier due to both disturbing sources. On the other hand, voltage processing amplifiers have a high input impedance, approaching infinity. The total disturbing voltage at the input terminals of the amplifier can now be determined using Fig. 2.6d.

The magnitude of the voltage source  $u_{dist}$  and the current source  $i_{dist}$  are given by (Paul 1992)

$$u_{dist} = j\omega\mu_0 A \vec{H} \quad (2.4)$$

and

$$i_{dist} = -j\omega C A \vec{E}, \quad (2.5)$$

respectively. Parameter  $A$  is the loop area given by the product of the length ( $\mathcal{L}$ ) of the two-wire line and the distance between the conductors  $d$ .  $\vec{H}$  and  $\vec{E}$  are the magnetic and electric field components of the plane wave, respectively. The angular frequency of the plane wave is represented by  $j\omega$  ( $j = \sqrt{-1}$ ) and  $C$  is the capacitance per meter and follows from Table 2.1.

The orientation of the current source,  $i_{dist}$ , is as depicted in Fig. 2.6. The orientation of the voltage source,  $u_{dist}$ , should be chosen such that the current resulting from this source generates a magnetic field that opposes the incident magnetic field (Paul 1992). The orientation of  $u_{dist}$  in Fig. 2.6b–d thus complies with an electromagnetic field orientation as shown in Fig. 2.6a.

From the electric field the magnetic field can be calculated, by dividing it by the wave impedance ( $Z_w$ )

$$H = \frac{E}{Z_w}. \quad (2.6)$$

Using Fig. 2.6d and e and Eqs. (2.4) and (2.5), the total disturbing signal due to an interfering plane wave can be determined.

$$u_{dist,tot} = i_{dist} \frac{R_s + j\omega L_d (1 + j\omega R_s C_s)}{1 + j\omega R_s C_s + j\omega C_d (R_s + j\omega L_d (1 + j\omega R_s C_s))} + u_{dist} \frac{j\omega L_d (1 + j\omega R_s C_s)}{1 + j\omega R_s C_s + j\omega C_d (R_s + j\omega L_d (1 + j\omega R_s C_s))} \quad (2.7)$$

and

$$i_{dist,tot} = i_{dist} \frac{R_s}{R_s + j\omega L_d [1 + j\omega R_s (C_s + C_d)]} + u_{dist} \frac{j\omega L_d [1 + j\omega R_s (C_s + C_d)]}{R_s + j\omega L_d [1 + j\omega R_s (C_s + C_d)]}. \quad (2.8)$$

The signal-to-disturbance ratio follows from  $20 \log (u_s/u_{dist,tot})$  and  $20 \log (i_s/i_{dist,tot})$ , respectively.

Equation (2.7) for the voltage processing amplifier is dominated by the  $u_{dist}$  term, at least at lower frequencies. At higher frequencies, typically at the edge of validity of the model,  $i_{dist}$  can not be neglected anymore. However, for the major part of the frequency range it holds that  $u_{dist}$  determines  $u_{dist,tot}$ . Since  $u_{dist}$  is determined by the magnetic field, it can be concluded that voltage processing amplifiers are more susceptible to the magnetic field rather than the electric field component of the plane wave.

For the current processing amplifier, the dual case is found. Current source  $i_{dist}$  dominates Eq. (2.8) which depends on the electric field. Therefore, it can be concluded that current processing amplifiers are more susceptible to the electric field rather than to the magnetic field component of the plane wave.

Figure 2.8 shows the transfer ( $H_{pw}$ ) of a plane wave to  $u_{dist,tot}$  (dotted line). The interconnect is a two-wire ribbon cable with  $d = 1.27$  mm,  $r_w = 190.5$   $\mu$ m and  $\mathcal{L}_{con} = 20$  cm. Source resistance is  $R_s = 10\Omega$  and  $C_s = 1$  pF. Up to approximately 150 MHz the interconnect can be regarded as electrically small. At 150 MHz the deviation of transfer  $H$  with the transfer obtained with the transmission line theory (Sect. 2.6.2) is about 2 dB. For lower frequencies, transmission line theory and the method presented in this section give the same results. The method presented in this subsection is, however, simpler.

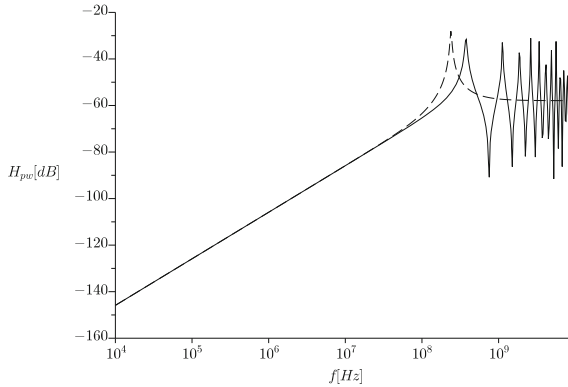


**Fig. 2.8** Transfer  $H_{pw}$  of a plane wave to a disturbing voltage at the input of a voltage processing amplifier. The orientation of the plane wave is depicted in Fig. 2.7. The interconnect is a two-wire ribbon cable with  $d = 1.27$  mm,  $r_w = 190.5$   $\mu\text{m}$  and  $\mathcal{L}_{\text{con}} = 20$  cm. Source resistance is  $R_s = 10\Omega$  and  $C_s = 1$  pF. The solid line is obtained with transmission line theory, the dashed line with the lumped model

### 2.6.2 Plane Wave Coupling to Large Interconnects

An interfering plane wave generates a disturbing current and voltage at the input terminals of the amplifier, see Fig. 2.7. Under the condition that  $d \leq \frac{\lambda}{2\pi}$  holds, current  $i_{in}$  and voltage  $u_{in}$  can be calculated with (Smith 1977; Flintoft 2013):

$$i_{in}(\omega) = \frac{1}{D} \int_0^{\mathcal{L}} K(l, \omega) [Z_0 \cosh \gamma l + Z_s \sinh \gamma l] dl + \frac{Z_0}{D} \int_0^d E_x^i(x, 0, \omega) dx - \frac{1}{D} [Z_0 \cosh \gamma \mathcal{L} + Z_s \sinh \gamma \mathcal{L}] \int_0^d E_x^i(x, l, \omega) dx \quad (2.9)$$

$$D = (Z_0 Z_s + Z_0 Z_{in}) \cosh \gamma \mathcal{L} + (Z_0^2 + Z_s Z_{in}) \sinh \gamma \mathcal{L}$$

$$u_{in}(\omega) = i_{in}(\omega) Z_{in},$$

where  $Z_0$  is the characteristic impedance of the interconnect,  $Z_s$  is the source impedance,  $Z_{in}$  is the input impedance of the amplifier,  $E_x^i(x, 0, \omega)$  is the electric field in the  $x$  direction (directed from the lower conductor to the upper conductor) incident on the source terminals,  $E_x^i(x, l, \omega)$  the field in the  $x$  direction incident on the  $Z_{in}$  terminals,  $\mathcal{L}$  is the length of the conductors,  $\omega$  is the radial frequency of the field, and  $\gamma$  is the propagation constant of the line.  $K(l, \omega)$  is the difference between the incident fields:  $K(l, \omega) = E_l^i(d, l, \omega) - E_l^i(0, l, \omega)$ , where  $E_l^i(d, l, \omega)$  is the field incident in the length direction on the upper conductor and  $E_l^i(0, l, \omega)$  is the field in the length direction incident on the lower conductor. Note that for the orientation of the plane wave in Fig. 2.7,  $K$  is zero since  $E_l$  is zero.

Solving the integrals for the field orientation depicted in Fig 2.7, results in:

$$\begin{aligned}
i_{in}(\omega) = & E_x^i d \frac{Z_0}{D} \left\{ 1 - e^{-jk_0 \mathcal{L} \sin \Phi} \left( \cosh \gamma \mathcal{L} + \frac{Z_s}{Z_0} \sinh \gamma \mathcal{L} \right) \right\} \\
& - 2 \frac{E_l^i}{\gamma} \frac{Z_0}{D} \sinh \left( j \frac{k_0 d}{2} \sin \Psi \right) \left( \sinh \gamma \mathcal{L} + \frac{Z_s}{Z_0} (\cosh \gamma \mathcal{L} - 1) \right) \quad (2.10) \\
D = & (Z_0 Z_s + Z_0 Z_{in}) \cosh \gamma \mathcal{L} + (Z_0^2 + Z_s Z_{in}) \sinh \gamma \mathcal{L},
\end{aligned}$$

with  $k_0 = \frac{2\pi}{\lambda}$  being the wave number of the plane wave, and  $\Phi$  and  $\Psi$  are the angles that  $\vec{S}$  makes with the interconnect.

Typically, disturbances at the termination on the amplifier side will show a 20 dB/dec increase with frequency. Anti-resonance points (i.e., maxima in the disturbance) and resonance points (minima) may occur. The first anti-resonance point typically gives the largest value of the disturbance and can be found at  $f_p = \frac{v}{4\mathcal{L}}$  in case of resistive line termination, with  $v$  being the velocity of propagation on the line. The other anti-resonance and resonance points are found at  $f_{ar} = n f_p$  and  $f_r = (n - 1) f_p$ , respectively, with  $n = 3, 5, 7 \dots$ . The exact resonance and anti-resonance frequencies may be shifted by a few percent when the terminations are formed by complex impedances instead of resistances.

Attenuation factor  $\alpha$  increases with frequency, thus increasing  $\gamma$ , and causes the depths of the anti-resonance points and the heights of the resonance points to be diminished (Smith 1977). For this reason it may be expected that in practical cases  $f_p$  will indeed give the frequency at which maximal disturbance will occur.

Figure 2.8 shows with the solid line the transfer  $H_{pw} = u_{in}/E$  for the interconnect presented in Sect. 2.6.1. Another example of the application of the presented equations can be found in (Flintoft 1999a,b), in which the disturbance induced in two-wire lines, twisted pairs, etc., by GSM phones is investigated using (among others) the method presented in this subsection.

### 2.6.3 Design for Low Plane Wave Coupling

The simplest and most straightforward measure that can be taken is to keep dimensions of the interconnect small. As long as the interconnect is electrically-small, the disturbance is inversely proportional to  $\mathcal{L}$ , i.e., a reduction of  $\mathcal{L}$  of a factor two will also reduce the disturbance by a factor two. Moreover, a small distance ( $d$ ) between the conductors causes lower values of  $u_{dist}$  and  $i_{dist}$ . The inductance of the interconnect decreases and the capacitance increases with decreasing distance. Designing (electrically-large) interconnects with a low value of  $Z_0 = \sqrt{L/C}$  is thus beneficial.

Electrically-large interconnects may be designed such that the attenuation factor  $\alpha$ , which forms the real part of  $\gamma$ , is large. This may be accomplished by designing for a relatively high conductor resistance, by selecting material with a high specific resistance, and a high value of the conductance  $G$  of the insulation between the

conductors.<sup>7</sup> Since  $\alpha$  increases with frequency, the beneficial effect on the transfer of interfering plane waves increases with frequency.

Higher values of the interconnect resistance and capacitance may, however, decrease the bandwidth of the interconnect too much, causing a distorted intended signal. Moreover, a higher value of  $R$  may decrease the signal to error ratio. A trade-off between the beneficial and detrimental effects of decreasing  $d$  and increasing  $R$  should be made in that case.

Another measure that can be taken is to prevent plane waves reaching the interconnect using shielding, e.g., by using a single conductive (ground) plane or a complete conductive enclosure. Shielding is discussed in Sect. 2.8. More about the positive effect of a conductive plane near an interconnect can be found in (Smith 1977; Reitsma 2005).

## 2.7 Differential and Common-Mode Disturbances

When disturbing signals are induced in an interconnect formed by, e.g., a wire over a conductive plane or a microstrip line, the disturbance is a differential signal and processed by the signal path comparable to the intended signal. When, however, an interconnect is placed over a conductive plane (which often occurs), a disturbance is generated in the path formed by the conductive plane and the interconnect aside from the differential signal. This disturbance is called a common-mode disturbance, because it causes signals that are equal in magnitude and have the same direction (Paul 1992) in both conductors of the interconnect. Common mode and differential-mode disturbances are elucidated in Fig. 2.9a.

The common-mode disturbances can be found by using the same principles as discussed in Sect. 2.6, but now it is assumed that the conductor spacing in the interconnect is negligible compared with the distance between the interconnect and ground plane. All conductors in the interconnect are treated as a single wire with a diameter equal to the overall diameter of the interconnect. The disturbances found in this loop form the common-mode disturbances in the interconnect, which are assumed to divide equally among the conductors in the interconnect (Smith 1977). This is modelled in Fig. 2.9b.

Although Figs. 2.9a and b present a representation valid for small interconnects, the discussion also holds for long interconnects. In the latter case, the common-mode currents at the terminals of  $Z_{in}$  are of concern.

Note that the effective disturbing signal sources driving the common-mode disturbances are determined for a distance,  $d_1$ , to the ground plane that is much larger than the distance,  $d_2$ , between the conductors in the interconnect. Hence, the common-mode disturbances induced on the interconnect are much greater than

---

<sup>7</sup> Note that these recommendations are the opposite of the general case in which the intended signal has to be transferred and hence  $\alpha$  should be as low as possible.

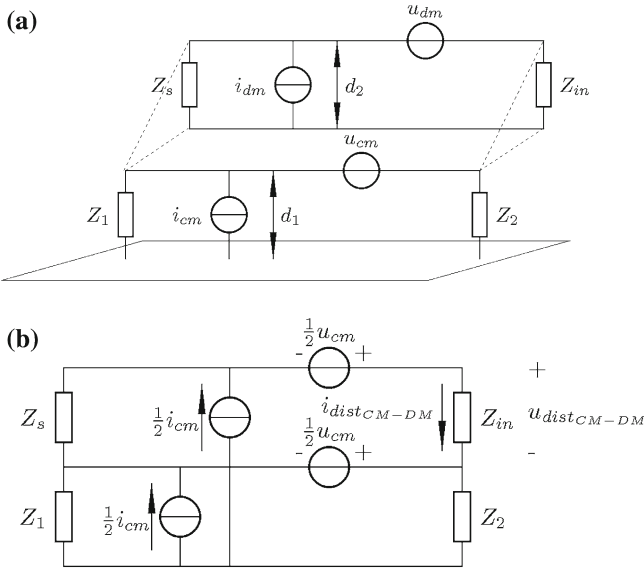


**Fig. 2.9** An interconnect is placed over a conductive plane. Differential-mode disturbances are generated in the path formed by both conductors of the interconnect,  $Z_s$ , and  $Z_{in}$ . Common-mode disturbances are generated in the path formed by the conductive plane, impedances  $Z_1$  and  $Z_2$  and the interconnect. **a** The interconnect between  $Z_s$  and  $Z_{in}$  is connected via  $Z_1$  and  $Z_2$  to a conductive plane. Both common mode and differential-mode disturbance are induced in the interconnect. Note that usually holds  $d_1 \gg d_2$ . **b** common-mode signals on interconnect

the differential-mode disturbances Flintoft 2013; Smith 1977. The total disturbance at the terminals of the amplifier, i.e., at  $Z_{in}$  can now be evaluated.

The impedances  $Z_1$  and  $Z_2$  determine the total disturbance. Their effect is considered for the extremes of zero and infinite impedance. Four combinations are possible and they are evaluated for each of these four cases for both voltage and current processing amplifiers in Table 2.2. The disturbance voltage in the case of a voltage processing amplifier and the disturbing current in the case of a current processing amplifier are denoted  $u_{distCM-DM}$  and  $i_{distCM-DM}$ , respectively. Just like in the previous cases,  $Z_s$  represents the source impedance and  $Z_{in}$  represents the input impedance of the amplifier.<sup>8</sup>

When both  $Z_1$  and  $Z_2$  are infinite, the common-mode signals cancel in  $Z_{in}$  (and  $Z_s$ ) and no disturbing signal occurs (Smith 1977). This is equivalent to a balanced input.

When either  $Z_1$  or  $Z_2$  is zero, and the other infinite, only the common-mode currents will generate a disturbance. This is because making either  $Z_1$  or  $Z_2$  zero, short circuits the  $i_{cm}/2$  current source of the conductor that is short circuited. Both

<sup>8</sup> The model with the common-mode sources divided equally over both connectors as shown in Fig. 2.9b can also be used to determine common-mode to differential-mode conversion for other cases of imbalance, e.g., when  $Z_{in}$  is also loaded by an impedance at its top terminal.

**Table 2.2** Common-mode to differential-mode conversion due to impedances  $Z_1$  and  $Z_2$ 

| $Z_1$    | $Z_2$    | $u_{distCM-DM}$  | $i_{distCM-DM}$  |
|----------|----------|--|--|
| $\infty$ | $\infty$ | 0  | 0  |
| $\infty$ | 0        | $\frac{i_{cm}}{2} \frac{Z_{in} Z_s}{Z_s + Z_{in}} \approx \frac{i_{cm}}{2} Z_s$  | $\frac{i_{cm}}{2} \frac{Z_s}{Z_s + Z_{in}} \approx \frac{i_{cm}}{2}$   |
| 0        | $\infty$ | $\frac{i_{cm}}{2} \frac{Z_{in} Z_s}{Z_s + Z_{in}} \approx \frac{i_{cm}}{2} Z_s$  | $\frac{i_{cm}}{2} \frac{Z_s}{Z_s + Z_{in}} \approx \frac{i_{cm}}{2}$   |
| 0        | 0        | $\frac{u_{cm}}{2} \frac{Z_{in}}{Z_s + Z_{in}} + \frac{i_{cm}}{2} \frac{Z_s Z_{in}}{Z_s + Z_{in}}$<br>$\approx \frac{u_{cm}}{2} + \frac{i_{cm}}{2} Z_s$ | $\frac{u_{cm}}{2} \frac{1}{Z_s + Z_{in}} + \frac{i_{cm}}{2} \frac{Z_s}{Z_s + Z_{in}}$<br>$\approx \frac{u_{cm}}{2} \frac{1}{Z_s} + \frac{i_{cm}}{2}$ |

common-mode voltages  $u_{cm}/2$  are unaffected by the short circuit and cancel each other because they have the same sign.

When both  $Z_1$  and  $Z_2$  equal zero, both common-mode current and common-mode voltage determine the disturbing input quantities. Because the conductor is short circuited at both sides, both the lower common-mode current source and the lower common-mode voltage source are short circuited. It should be noted that  $u_{cm}/2$  may be significantly larger than  $i_{cm}/2$  (see, e.g., Eqs. (2.4) and (2.5)). Both  $u_{distCM-DM}$  and  $i_{distCM-DM}$  are typically dominated by  $u_{cm}/2$ .

Of course in practical situations neither  $Z_1$  nor  $Z_2$  will be zero or infinite. Using the models, the effect of different values of  $Z_1$  and  $Z_2$  between these extremes can readily be analyzed.

### 2.7.1 Decreasing the Common-Mode Disturbance

The common-mode signals that are transferred to a differential total disturbance signal can be significantly decreased. Minimizing height  $d_1$  is a simple and effective method.

Using a shielded cable as interconnect, e.g., a shielded two-wire, also decreases the common-mode signals. The common-mode signals are, ideally, confined within the shield and no conversion to a differential-mode disturbance signal at the input of the amplifier occurs. Shielded cables are, however, not ideal and some coupling to the amplifier input may still occur. See for instance, Sect. 2.8.2 and (Goedbloed 1993; Ott 1998, 2009). At the boundary of the interconnect and the amplifier, the shield should be connected to a highly conductive plate or enclosure. This shielding plate or enclosure forms a boundary between the common-mode signals and the amplifier. Sometimes a shield is called a current boundary for this reason (Buesink 1996).



Common-mode chokes are often recommended (Ott 1998, 2009; Reitsma 2005; Goedbloed 1993) because they effectively suppress a common-mode signal, while not affecting differential (i.e., the intended) signals (Ott 1998). A common mode choke may result in considerable reduction of the disturbance in the frequency range where it is effective, which may be limited up to, e.g., 30 MHz (Ott 1998).

When the effect of a common-mode choke is evaluated for the situation depicted in Fig. 2.9b (and with the earlier presented combination of values of  $Z_1$  and  $Z_2$ ) it is found that it is only effective when both  $Z_1$  and  $Z_2$  are zero. It nullifies the  $u_{cm}/2$  disturbance, but it does not affect the disturbance caused by  $i_{cm}/2$ .

## 2.8 Shield Design

The disturbance from interfering sources can usually be reduced significantly when shielding with good conductive material is applied. Shield design is therefore dealt with briefly in this section. Appendix A presents a more in depth discussion.

The equations used to design the shield are taken from the work of Kaden 1959. In this work elaborate equations are presented for calculating shielding factors,  $\mathcal{S}$ , of conducting structures. These structures are: two (infinite) parallel plates, the cylinder, and the sphere. The cylinder can be used to calculate the shielding factor of, e.g., a solid coax cable. The sphere is regarded as a good approximation for other three dimensional structures (enclosures) of the same volume. Shielding factor  $\mathcal{S}$  is determined by both the shielding factor for magnetic,  $\mathcal{S}_H$ , and for electric fields,  $\mathcal{S}_E$ .

Shield design can in principle be straightforward. The shielding factor depends on the radius of the cylinder or the sphere ( $r_0$ ), with respect to the wavelength of the interfering field, and the skin effect. In the region where  $\lambda \gg r_0$ , the shielding is determined by the conductor properties. When  $r_0$  is of the same order of magnitude as (or larger than)  $\lambda$ , ‘shielding breakdown’ due to resonances occur. Shielding breakdown occurs at different frequencies for  $\mathcal{S}_H$  and  $\mathcal{S}_E$ . Material that absorbs the EM energy can be used in this region to decrease the adverse effect of shielding breakdown. We will not elaborate on this. In this work the maximal frequency or maximal dimensions where the shield is effective will be determined.

Here, the following design strategy is proposed:

1. determine the conductor thickness for adequate  $\mathcal{S}$  at the lowest interfering frequency
2. determine the maximum  $r_0$  to prevent ‘shielding breakdown’ at the highest interfering frequency, or determine this frequency for a given  $r_0$

Since  $\mathcal{S}_H$  can be expected to determine  $\mathcal{S}$  in case of  $r_0 \ll \lambda$  ( $\mathcal{S}_H \ll \mathcal{S}_E$ , see Fig. A.1 P.276, up to approximately 3 MHz), it suffices to design the shield for a certain minimal value of  $\mathcal{S}_H$  at the lowest interfering frequency to be expected. Since  $\mathcal{S}_H$  is determined by the attenuation of the magnetic field ( $a_s$ ) in this frequency region (see appendix A),  $\mathcal{S}_H$  increases with frequency, resulting in an even greater

shielding factor for frequencies higher than designed for.  $\mathcal{S}_E$  will automatically be sufficient also.

The required shield thickness,  $d$ , for a specified amount of  $a_s$  (e.g.,  $20 \log |a_s| = 40 \text{ dB}$ ) and at a given frequency depends on the skin depth ( $\delta = \sqrt{2\rho/(\mu\omega)}$ ), and can be approximated by

$$d \approx \begin{cases} a \frac{\mu_r \delta^2}{2r_0} \sqrt{10^{\left(\frac{a_s}{10}\right)} - 1} & d < \delta \text{ ('low frequencies')} \\ \delta \left[ \ln \left( \frac{a \sqrt{2} \delta \mu_r}{r_0} \cdot 10^{\left(\frac{a_s}{20}\right)} \right) \right] & d > \delta \text{ ('high frequencies')}, \end{cases} \quad (2.11)$$

which is derived from Eq. (A.2), see P.275. The constant  $a$  equals 2 in the case of a cylinder and 3 in the case of a sphere.

Resonances in shielding (breakdown) are modelled by a correction factor ( $a_m$ ). The shielding factor for magnetic fields is given by  $\mathcal{S}_H = 20 \log |a_s| + 20 \log |a_m|$ . The shielding factor for electric fields is  $\mathcal{S}_E = 20 \log |a_s| + 20 \log |a_E|$ . Correction factor  $a_E$  models both low and high-frequency electric field attenuation. Equations for both  $a_E$  and  $a_m$  are presented in appendix A.

The maximal dimensions of the shield should be smaller than the wavelength corresponding to the first resonance frequency, to prevent 'shielding breakdown' due to resonances. An unacceptable decrease of  $\mathcal{S}$  due to the frequency dependency of  $a_E$  or  $a_m$ , can be prevented by taking a slightly larger wavelength as lower limit. For cylindrical conductors, it is recommended to have a maximal radius of  $r_0 = 0.25\lambda$ , while for a spherical conductor a maximal radius of  $r_0 = 0.4\lambda$  is recommended, and for a cube the maximal  $a = 0.797\lambda$  is found (Kaden 1959).

For example, Eq. (2.11) results in a thickness of 0.11 mm for a required  $\mathcal{S}_H$  of 85 dB at 1 MHz for a copper sphere with  $r_0 = 1 \text{ m}$ . Proper shielding can be expected up to 120 MHz. When we have a copper cylinder with a radius of 6 cm and want to achieve a  $\mathcal{S}_H$  of 40 dB at 30 kHz, a thickness  $d$  of 0.24 mm is found (Kaden 1959). Up to 1.25 GHz there is proper shielding.

### 2.8.1 Shield Design Considerations

Factor  $20 \log |a_s|$  gives rise to extremely large attenuation values for frequencies higher than, e.g., 10 MHz. In practice, these large attenuation values are not reached, since the necessary openings for interconnect feed through limit the reachable attenuation. Kaden proposes to use an upper limit of 12 Np (i.e., 104 dB) (Kaden, 1959) since larger attenuations are hardly verifiable by measurements (van der Laan 2002). This upper limit is used when calculating  $\mathcal{S}_H$  and  $\mathcal{S}_E$  in Fig. A.1 (Kaden 1959).

Apertures in the enclosure are inevitable, so the practical upper limit makes sense. In order to maintain a high practical upper limit, one has to take care that currents can flow as unaffected by the apertures as possible. Large round apertures and slits do affect the current flow in the shield and therefore the shielding factor is reduced.

It is better to use many small round holes instead of one big one for, e.g., cooling purposes (Paul 1992). A slit reduces the homogeneity of the current flow and a voltage is induced over the slit. Therefore electric and magnetic fields can enter the enclosure. In case of round holes, this also occurs, but now the current flow is much more homogeneous and therefore much less electric and magnetic energy enters the enclosure (Goedbloed 1993). Apertures that are inevitable should therefore be round.

Holes in the enclosure should preferably be realized as cylinders perpendicular to the enclosure (Kaden 1959). The attenuation ('Kamindämpfung'; 'Kamin' or 'chimney' damping) of these cylinders is  $a_{k_E} = 20.85 \frac{l}{r_0}$  [dB] for electric fields and  $a_{k_H} = 15.98 \frac{l}{r_0}$  [dB] for magnetic fields, with  $l$  being the length of the cylinder and  $r_0$  the radius of the cylinder.<sup>9</sup> Cylinders with an  $\frac{l}{r_0}$  ratio of 6–8 will thus provide enough attenuation (van der Laan 2002). The diameter of the cylinder should remain several times smaller than the wavelength of the interfering fields, in order to remain a waveguide beyond cut-off (van der Laan 2002). The corner wavelength for a cylindrical waveguide beyond cut-off is  $\lambda_c = \frac{2\pi r_0}{1.841}$  (Goedbloed 1993); the equations for the 'Kamindämpfung' are thus valid as long as  $\lambda \gg \lambda_c$ .

For additional practical guidelines in realizing and building shielding enclosures, the reader is referred to readily available EMC textbooks, e.g., (Goedbloed 1993; Ott 1998, 2009).

## 2.8.2 Surface Transimpedance

When the signal paths (interconnects) and source and load are completely shielded, ideally no undesired EM coupling from external signal paths exists. This would be true when the shield is ideal, i.e., it would be a perfect conductor. Since the shield is not a perfect conductor (because, e.g., holes are present) currents induced by EM fields will penetrate the shield and produce a voltage distribution along the inside length of the shield. This voltage distribution in turn produces a current in the interior source and load impedances (Smith 1977).

A typical way of calculating the EM coupling through a shield is to first calculate the current induced on the shield exterior by the incident field, assuming that the shield is a perfect conductor and completely encloses the internal signal path (Paul 1992). This shield current,  $i_{sh}$  diffuses through the shield wall to give a voltage drop on the *interior surface of the shield*,  $du_{dist} = i_{sh} Z_t dx$ .  $Z_t$  is called the transfer impedance in EMC literature, e.g., (Goedbloed 1993; Paul 1992; Williams 1996). Electronics engineers are more familiar with the name transimpedance to describe a current to voltage transfer ( $u_{dist} = i_{sh} Z_t$ ). In this work the name transimpedance will therefore be used. Equivalently, a disturbing current inside a shield due to a voltage across the shield and the reference, may be calculated by using the concept of transadmittance ( $Y_t$ ); transfer admittance in EMC literature. The current is given

---

<sup>9</sup> Kaden points out that the equations for the Kamindämpfung are accurate when  $l$  is larger than or of the same magnitude as  $r_0$ .

by  $i_{dist} = u_{sg} Y_t$ , where  $u_{sg}$  is the voltage between the shield and the reference conductive plane.

The approach of calculating a disturbing voltage inside a shield by using the concept of  $Z_t$  is equally valid for any shield, e.g., coax, triax, shielded pair, shielded multi-conductor, shielded multicoax, etc. (Smith 1977), but it may, for instance, also be used in pcb design and grounding (van Horck 1998; van Helvoort 1995).

Solid coaxial shields usually show a low  $Z_t$ . For a solid cylindrical shield around an interconnect,  $Z_t$  in [ $\Omega/m$ ] is (Kaden 1959; Paul 1992)

$$Z_t = \frac{1}{\sigma \pi D_m d} \frac{d^{\frac{1+j}{\delta}}}{\sinh d^{\frac{1+j}{\delta}}}, \quad (2.12)$$

with  $D_m = 2r_0$  being the inner diameter of the shield,  $d$  the shield thickness, and  $\sigma = 1/\rho$  the conductance of the material. For shield thicknesses less than a skin depth,  $d \ll \delta$ , the transimpedance reduces to the resistance  $R_t = \frac{1}{\pi \sigma D_m d}$  since the shield current can completely diffuse to the interior of the shield. For wall thicknesses greater than a skin depth, the current on the exterior of the shield only partly diffuses through the shield wall, and  $Z_t$  decreases with increasing frequency. The interior and exterior of the shield are becoming isolated due to the skin effect. For a completely closed cylinder (e.g., a copper cylinder),  $Z_t$  will soon become negligibly small for frequencies at which the skin depth is effective.

When we have a braided shield, holes are present in the shield through which EM fields may leak. This causes  $Z_t$  to become inductive.<sup>10</sup> For instance,  $Z_t$  may be approximated by  $Z_t \approx j\omega\mu_0 \frac{2}{3\pi^2} \frac{pr_o}{0.5D_m}$  (Kaden 1959) in case of circular holes,

with  $r_o$  being the radius of the holes and  $p = \frac{vr_o^2}{D_m}$ . Parameter  $v$  is the number of holes across the length  $\mathcal{L}$  of the braid. Equations for calculating the effects of the properties of the braid on  $Z_t$  for practical coax cables, can be found in (Kley 1993). The equation for  $Z_t$  presented here is, however, simple and general design rules follow from it. It shows that  $Z_t$  for a given  $p$  increases with increasing  $r_o$ . Moreover, a large number of small holes is better than a small number of large holes, under the assumption that the total area remains equal (Kaden 1959).

### 2.8.3 Shielded Electrically-Small Systems

Sometimes it is impossible to reduce the dimensions of an interconnect enough to obtain acceptable levels of disturbance. This may be the case when, e.g., another design requirement demands the interconnect to have some minimum dimensions

<sup>10</sup> Typically at approximately 1 MHz,  $Z_t$  will become dominated by the inductances according to graphs of  $Z_t$  for various types of coax cables and shielded cables in (Goedbloed 1993) and (Ott 1998).

that are too large from an EMI point of view. Reduction of the disturbance can now be obtained by shielding the system.

The disturbing signal source at the input of amplifiers can be determined by calculating the shield current ( $i_{sh}$ ) and multiplying it with  $Z_t$ . An equation for  $i_{sh}$  is derived for a plane wave oriented as depicted in Fig. 2.7 from the transmission line equations presented in (Smith 1977). For other field directions the reader is referred to (Smith 1977), but similar results can be expected. The shield current can be calculated from the average voltage that is induced across the shield by the EM-field. The average voltage that is induced is given by (Smith 1977)

$$u_{sha} = E_x \frac{h}{2} (1 - e^{-jk_0 \mathcal{L}}) \mathcal{L}, \quad (2.13)$$

with  $h$  being the height of the shielded interconnect above a conductive plane, and  $k_0 = 2\pi/\lambda$  being the wave number.<sup>11</sup> Since the shield is electrically short,  $k_0 \mathcal{L} < 1$ , it was found (using the method described in (Paul 1992)) that this equation can be very well approximated by<sup>12</sup>

$$u_{sha} \approx j\omega\mu_0 H \mathcal{L} h, \quad (2.14)$$

which is similar to Eq. 2.4.

The shield current can now be determined with  $i_{sh} = u_{sha} Y_t$ . Transadmittance  $Y_t$  can be determined from Fig. 2.3c, when low termination impedances  $Z_1$  and  $Z_2$  are assumed, which is the recommended case (Goedbloed 1993). For  $Y_t$  is found

$$Y_t = \frac{1}{Z_2 + j\omega \frac{L_{sh}}{2} + \frac{Z_1 + j\omega \frac{L_{sh}}{2}}{1 + j\omega C_{sh} (Z_1 + j\omega \frac{L_{sh}}{2})}}. \quad (2.15)$$

Shield parameters  $L_{sh}$  and  $C_{sh}$  can be calculated using the equations presented in Table 2.1 (second row).

The disturbance voltage source ( $u_{dist,sh}$ ) that appears at the input of the amplifier (see Figs. 2.6d and e) can now be determined. This voltage source equals  $u_{dist,sh} = u_{sha} Y_{shield} Z_t$ . The total disturbing signal (either current or voltage) at the input of a current processing and voltage processing amplifier can now be determined using Eqs. (2.7) and (2.8). The lumped parameters  $L_d$  and  $C_d$  are those of, e.g., coax.

<sup>11</sup> For an electrically-small system holds  $\mathcal{L} \leq 0.1\lambda$ , resulting in a maximal wave number of  $2\pi/(10\mathcal{L})$ .

<sup>12</sup> Comparison of both equations showed a deviation of less than 2 % for short shields.

Since  $u_{sha}$  has a zero in the origin,  $i_{sh}$  increases at a rate of 20 dB/dec up to the pole in  $Y_{shield}$ , after which it remains constant.<sup>13</sup> Disturbance voltage source  $u_{dist,sh}$  equals  $u_{sha}Y_{shield}Z_t$ .

Compared to an unshielded interconnect with the same dimensions and height as a shielded one,  $u_{dist,sh}$  appears to be a factor (the shielding factor) lower. This shielding factor may be approximated by

$$\mathcal{S} = \frac{u_{dist}}{u_{dist,sh}} \approx \frac{Z_1 + Z_2 + j\omega L_{sh}}{Z_t}. \quad (2.16)$$

For a high  $\mathcal{S}$ , the transimpedance  $Z_t$  should be as small as possible. The inductive part of  $Z_t$  should at least be much (e.g., 100 times) smaller than  $L_{sh}$ .

Although high values of the terminating impedances  $Z_1$  and  $Z_2$  seem beneficial ( $Z_1$  and  $Z_2$  in Fig. 2.3c), effort has to be made to keep them as low as possible, since high terminating impedances may cause capacitive coupling of a disturbance. This means that, e.g., pigtailed to terminate the shield have to be avoided since they cause  $Z_1$  and  $Z_2$  to become inductive and hence deteriorate  $\mathcal{S}$  with increasing frequency. Apart from that, direct inductive and capacitive coupling to the interior shielded wire over the length of the pigtail section occurs (Paul 1992).

## 2.8.4 Shielded Electrically-Large Systems

The design recommendations given in the section about shielded electrically-small systems also hold for large systems. The main difference encountered is that reflections in the shield may occur that degrade the shielding.

In case of a lossless shield, the current and voltage at the input of the amplifier is calculated with (Smith 1977)

$$\begin{aligned} i_{in} &= E_x h \frac{Z_t \mathcal{L}}{PD} \int_0^{\mathcal{L}} \left[ \left\{ (Z_0 - Z_1) \sin k_0 \mathcal{L} \sin k_0 l + j(Z_0 + Z_2) \sin k_0 \mathcal{L} \cos k_0 l \right. \right. \\ &\quad \left. \left. - j(Z_1 + Z_2) \cos k_0 \mathcal{L} \sin k_0 l \right\} \cdot \{Z_c \cos k_{0i} l + jZ_s \sin k_{0i} l\} \right] dl \quad (2.17) \\ P &= (Z_c Z_s + Z_c Z_{in}) \cos k_{0i} \mathcal{L} + j(Z_c^2 + Z_s Z_{in}) \sin k_{0i} \mathcal{L} \\ D &= (Z_0 Z_1 + Z_0 Z_2) \cos k_0 \mathcal{L} + j(Z_0^2 + Z_1 Z_2) \sin k_0 \mathcal{L} \\ u_{in} &= i_{in} Z_{in}, \end{aligned}$$

<sup>13</sup> At frequencies lower than the pole, the results of this equation are the same as will result from the transmission line approach (Smith 1977) that will be presented in Sect. 2.8.4. For frequencies where  $i_{sh}$  remains constant, it is overestimated with an amount dependent on  $h$ . It was found that up to an  $h = 50$  cm the overestimation is about 6 dB. Smaller heights result in smaller overestimations. This is acceptable.

under assumption of a plane wave exiting the shield as depicted in Fig. 2.7. With  $h$  being the height of the shield over the conductive plane,  $Z_0$  being the characteristic impedance of the shield treated as a single wire over a conductive plane,  $Z_1$  and  $Z_2$  being the termination impedances of the cable shields (also treated as a single wire over a conductive plane).  $\mathcal{L}$  is the length, and  $k_0 = 2\pi/\lambda$  is the wave number.  $Z_c$  is the characteristic impedance of the interconnect inside the shield, and  $k_{0i}$  is the wave number of the interconnect inside the shield.  $Z_s$  is the source impedance and  $Z_{in}$  is the load impedance of the interconnect, i.e., the input impedance of the amplifier.  $E_x$  is the electric field component parallel to the terminations of the shielded signal path. For other directions of the EM field the interested reader is referred to (Smith 1977).

At low frequencies, the equation given here gives the same result as the method presented in Sect. 2.8.3. Current  $i_{in}$  at the input terminals of the amplifier, shows a 20 dB/dec increase, which is consistent with the increase in  $Z_t$  with frequency. At higher frequencies, the resonance and anti-resonance points due to reflections are damped out when  $Z_1 = Z_2 = 0$  and  $Z_s = Z_{in} = Z_c$ . When either  $Z_1$  or  $Z_2$  is infinite, i.e., an open end occurs, resonances start to occur that decrease the effectivity of the shield (Smith 1977). The shield should thus be connected at both sides to the reference via low impedances.

To simplify the design of shielded long interconnects, the equations given in Sect. 2.8.3 can be used. After all, up to the frequency that the interconnect becomes long, both the method for small interconnects and the one for long interconnects give the same result. An electrically-small shield with an appropriate  $\mathcal{S}$ , may be expected to have an appropriate  $\mathcal{S}$  also when it becomes electrically-large as long as termination impedances  $Z_1$  and  $Z_2$  are low (zero). When the source impedance and the (input) impedance of the system (amplifier) are not matched to the characteristic impedance of the internal interconnect, reflections may occur that may increase the disturbance, as is the case for the unshielded long interconnect.

Better shielding behavior may be expected when the electrically-long shield is made electrically small by connecting it to the reference (ground) at multiple points spaced  $\leq \lambda/10$  from each other (Paul 1992). The shielding factor  $\mathcal{S}$  may then be estimated by using approximations valid for electrically-small systems.

## 2.9 Conclusions

The fidelity of the transfer of an amplifier is hampered by noise generated in the amplifier and by disturbances that may be in-band or out-of-band. This chapter deals with the interconnect properties. The interconnect properties may influence (low-pass filter) the transfer of the intended signal (e.g., from source to the amplifier) and determine the amount of disturbance coupled to the amplifier. These properties depend on the dimensions of the interconnect.

Equations that enable the designer to estimate the amount of disturbance coupled to the interconnect, and to determine the maximal dimensions of the intercon-

nect for both the intended signal and the disturbance are presented. The presented equations are valid for plane-wave (far-field) coupling to both electrically-short and electrically-large interconnects, under assumption that the distance between the conductors remains smaller than  $\lambda/(2\pi)$ . Cross-talk (near-field) coupling is not considered.

Both common-mode and differential-mode disturbance can occur. Since common-mode loops are usually larger than differential-mode loops, common-mode disturbance is usually larger also. Balancing the impedances that terminate the interconnects cancels the common-mode disturbance. Imbalances in these impedances causes common-mode to differential-mode conversion, thus increasing the total disturbance. A model and equations that can be used to analyze this effect are presented.

In general, it may be concluded that the smaller the dimensions of the interconnect, the smaller the disturbance coupled to it. Sometimes, other design requirements demand interconnect dimensions larger than allowed from a disturbance point of view. In that case, shielding may be applied. Equations to facilitate the design of shields (for both interconnects and enclosures) are also presented.

## References

- F.J.K. Buesink, Current boundaries reduce crosstalk between common-mode current loops, in *Symposium Electromagnetic Compatibility*, ch. 2, IEEE Student Branch Delft, 1996
- F.G. Canavero, S. Pignari, V. Daniele, *Susceptibility analysis of complex systems*, in *Proceeding of IEEE*, pp. 618–621, 1990
- I.D. Flintoft, Coupling of EMI to cables: theory and models, tech. rep., University of York (2013)
- I.D. Flintoft, Measurement of RF coupling to ethernet cables, tech. rep., University of York (1999a)
- I.D. Flintoft, Statistics of EMI on ethernet cables due to multiple GSM phones, tech. rep., University of York (1999b)
- J.J. Goedbloed, *Electromagnetic compatibility*, 1st edn. (Prentice Hall, New Jersey, 1993)
- H. Haase, Full-Wave Field Interactions of Nonuniform Transmission Lines. PhD thesis, Otto-von-Guericke-Universität Magdeburg, 2005
- H. Kaden, *Wirbelströme und Schirmung in der Nachrichtentechnik*, 2nd edn. Springer, Berlin, 1959. in German
- R. W. P. King, *The theory of linear antennas*, 1st ed. (Harvard University Press, Cambridge, MA, 1956)
- R.W.P. King, C.W. Harrison, *Antennas and Waves, a modern approach*, 1st edn. (The M.I.T. Press, Cambridge, MA 1969)
- T. Kley, Optimized single-braided cable shields. *IEEE Trans EMC* **35**, 1–9 (Feb. 1993)
- F.B.J. Leferink, Inductance calculations; experimental investigations, in *IEEE International Symposium on EMC*, pp. 235–240, 1996
- F.B.J. Leferink, Inductance calculations; methods and equations, in *IEEE International Symposium on EMC*, pp. 16–22, 1995
- F.B.J. Leferink, Inkoppeling en uitstraling bij interfaces, in *Postacademische Cursus Elektromagnetische Compatibiliteit*, ch. 10, PATO/TUE, 2002
- F.B.J. Leferink, Reduction of radiated electromagnetic fields by creation of geometrical asymmetry. PhD thesis, University of Twente, 2001
- F.B.J. Leferink, M.J.C.M. van Doorn, “Inductance of printed circuit board ground planes”, in *IEEE Int (Symp. on EMC, Dallas, 1993)*, pp. 327–329



- G.C.M. Meijer, *Elektronische Implementatiekunde*, 1st edn. (Delftse Universitaire Pers, 1996)
- S.J. Orfanidis, *Electromagnetic Waves and Antennas*. freely available at: <http://www.ece.rutgers.edu/~orfanidi/ewa>, 1st ed., 2004
- H.W. Ott, *Electromagnetic Compatibility Engineering*, 1st ed. (Wiley, New York, 2009)
- H.W. Ott, *Noise reduction techniques in electronic systems*, 2nd edn. (Wiley, New York, 1988)
- C.R. Paul, *Introduction to Electromagnetic Compatibility*, 1st edn. (Wiley, New York, 1992)
- G.P. Reitsma, *Design of Electromagnetically Compatible Electronics*. PhD thesis, Delft University of Technology, 2005
- W. Sinnema, *Electronic Transmission Technology, lines, waves, and antennas*, 2nd edn. (Prentice Hall, New York, 1988)
- A.A. Smith, *Coupling of external electromagnetic fields to transmission lines*, 1st edn. (Wiley, New York, 1977)
- P.C.T. van der Laan, “Afscherming”, in *Postacademische Cursus Elektromagnetische Compatibiliteit*, ch. 5, PATO/TUE, 2002
- M.J.A.M. van Helvoort, *Grounding Structures for the EMC-protection of cabling and wiring*. PhD thesis, Eindhoven University of Technology, 1995
- F.B.M. van Horck, *Electromagnetic Compatibility and Printed Circuit Boards*. PhD thesis, Eindhoven University of Technology, 1998
- T. Williams, *emc for product designers*, 2nd ed. (Reed educational and professional publishing Ltd., Oxford, 1996)

EMI-Resilient Amplifier Circuits

van der Horst, M.J.; Serdijn, W.A.; Linnenbank, A.C.

2014, XV, 307 p., Hardcover

ISBN: 978-3-319-00592-8